Wave induced Turbulence and Bubbles and their Effect on Radiance in the Upper Ocean

Svein Vagle
Ocean Sciences Division, Institute of Ocean Sciences
Sidney, BC, V8L 4B2, Canada
phone: (250) 363-6339 fax: (250) 363-6798 email: Svein.Vagle@dfo-mpo.gc.ca

Award Numbers: N000140710754 & N000140610379
http://www.opl.ucsb.edu/radyo/

LONG-TERM GOALS

The long-term goal of this project is to measure wave induced turbulence and bubble clouds at a range of atmospheric and oceanographic conditions, covering a wide range of bubble sizes and concentrations, and to investigate their effect on radiance in the upper ocean. This is as a response to the disturbing fact that despite the fundamental importance of optical backscatter in the ocean it is still not possible to explain more than 5 to 10 percent of the particulate backscattering in the ocean based on known constituents even during periods with no active wave breaking (Terrill & Lewis, 2004). An important part of this work is to improve on our understanding of the role of manmade and natural surfactants in modifying the turbulence and bubble fields and therefore ultimately the upper ocean radiance.

OBJECTIVES

The main objectives of this study where **1)** to develop the necessary technology to allow for in-situ measurements of bubble size distributions over a wide range of bubble sizes and with sufficient temporal and air-fraction resolution to investigate the role of bubbles on upper ocean radiance, **2)** develop and test methods and algorithms to obtain bubble size distributions from such instrumentation, **3)** to make comparisons between different bubble measurement techniques (acoustical and optical) to investigate strengths and limitations , **4)** to make observations of bubbles clouds at a range of atmospheric and oceanographic conditions, and **5)** to make measurements of ocean microlayer surfactants to investigate their role in modulating the bubble field.

APPROACH

Different acoustical techniques utilizing the resonant behaviour of small bubbles have for some time been used to obtain bubble size distributions in the ocean (e.g., Vagle and Farmer, 1998). These approaches make use of the fact that bubbles will resonate at a frequency proportional to their size and that the resulting scattering cross section of these bubbles is orders of magnitude higher than the corresponding geometrical scattering cross section from a particle of the same size. The freely flooding acoustical resonator, pioneered by H. Medwin allows bubble size measurements through inversion of the bulk acoustic properties of the fluid (Farmer, Vagle & Booth, 1998; 2005). In this project modified acoustical resonators were combined with a suite of other instruments, including dopbeam sonars for

Report Documentation Page

Form Approved
OMB No. 0704-0188

1. REPORT DATE	2. REPORT TYPE	3. DATES COVERED
30 SEP 2011		**00-00-2011 to 00-00-2011**

4. TITLE AND SUBTITLE	5a. CONTRACT NUMBER
Wave induced Turbulence and Bubbles and their Effect on Radiance in the Upper Ocean	5b. GRANT NUMBER
	5c. PROGRAM ELEMENT NUMBER
6. AUTHOR(S)	5d. PROJECT NUMBER
	5e. TASK NUMBER
	5f. WORK UNIT NUMBER
7. PERFORMING ORGANIZATION NAME(S) AND ADDRESS(ES) **Institute of Ocean Sciences,Ocean Sciences Division,Sidney, BC, V8L 4B2, Canada,**	8. PERFORMING ORGANIZATION REPORT NUMBER
9. SPONSORING/MONITORING AGENCY NAME(S) AND ADDRESS(ES)	10. SPONSOR/MONITOR'S ACRONYM(S)
	11. SPONSOR/MONITOR'S REPORT NUMBER(S)

12. DISTRIBUTION/AVAILABILITY STATEMENT
Approved for public release; distribution unlimited

13. SUPPLEMENTARY NOTES

14. ABSTRACT

15. SUBJECT TERMS

16. SECURITY CLASSIFICATION OF:			17. LIMITATION OF ABSTRACT	18. NUMBER OF PAGES	19a. NAME OF RESPONSIBLE PERSON
a. REPORT **unclassified**	b. ABSTRACT **unclassified**	c. THIS PAGE **unclassified**	**Same as Report (SAR)**	**9**	

measurements of upper ocean turbulence, an array of thermistors, backscatter sonars, and microlayer sampling, to investigate the upper ocean bubble field. These measurements were augmented with meteorological and oceanographic, as well as surface wave observations, collected by other RadyO investigators during three successful field campaigns in the surf zone off Scripps pier, and onboard the R/P FLIP and R/V Kilo Moana off Santa Barbara and off Hawaii in 2008 and 2009.

WORK COMPLETED

As a result of this project we now have several novel acoustical resonator systems capable of measuring bubbles with radii between 3 μm and approximately 350 μm in-situ once every second. The Scripps pier measurements gave us the opportunity to make simultaneous acoustical and optical measurements of the bubble field (Twardowski et al., 2011), and during the two RadyO field studies we collected several excellent data sets that have now been analysed. Also, during the development of this system we developed new and improved methods for inverting the measurements to obtain acoustical attenuation estimates as a function of frequency and subsequently the bubble size distribution. The main contributor to this work was Postdoctoral fellow Helen Czerski (Czerski et al., 2011a).

During the two ship-based field experiments we also collected a number of microlayer samples using both the glass plate technique (Wurl et al. 2009) and a small self-propelled microlayer sampler deployed from R/V Kilo Moana. The main contributor to the analysis of these data have been Postdoctoral fellow Oliver Wurl (Wurl et al. 2011a, 2011b).

RESULTS

To reach one of the main goals of this project (Objectives 1&2), namely to measure very small bubbles, it was desirable to extend the existing bubble population measurements to smaller radii. This requires attenuation measurements to be extended to higher frequencies. Although the principles of resonator operation do not change as the frequency increases, the assumptions previously made during the spectral analysis may no longer be valid. In order to improve on the methods used to calculate attenuation from acoustical resonator outputs Helen Czerski developed a more complete analysis of the acoustical resonator operation than had been previously published. This new approach allows for robust attenuation measurements over a much wider frequency range, and enables accurate measurements from lower-quality spectral peaks (Czerski et al., 2011a). By combining the new algorithms with the improved acoustical resonator technology, we now have a much improved system to measure a wide range of bubble populations in-situ.

During the Scripps-pier surf-zone experiment, the effects of particle fields including bubbles on the optical volume scattering function (VSF) were investigated (Twardowski et al., 2011). Inversion results exhibited stable solutions that qualitatively agreed with concurrent acoustical resonator measurements of bubbles, aggregate particle size distribution expectations, and anectodal evidence from the field (Objective 3).

Optical observations from air-borne or satellite-based sensors are becoming the major source of oceanic information about algal blooms, primary productivity, etc., and the need for calibrating these sensors using independent in-situ sensors is growing. Comparisons between acoustical and optical techniques could be made from simultaneous observations, by two independent instruments, of the bubble field behind R/V Kilo Moana as part of the ship-based observations in 2008 and 2009 (Czerski

et al. 2011b). The measurements agree well (Objective 3). Also, the observations allowed for an investigation into the coating of the bubbles by surfactants since both the optical and acoustical properties of bubbles are functions of the coating. The results suggest that the bubbles measured in this study had a coating with thickness of 10 nm and a refractive index of 1.8 and that the coating thickness is the more important parameter for optical inversions (Czerski et al. 2011b) (Objective 5).

During the field study south of Hawaii, simultaneous observations of upper ocean turbulence and bubble size distributions were used to study the role of stratification on turbulence dissipation rates and on the upper ocean bubble field (Objective 4). It is clear from our results that large positive heat flux and associated upper ocean thermal stratification have a significant effect on the turbulence kinetic energy near the ocean surface. Our results show an order of magnitude reduction in the turbulence dissipation rate ε during the period of the day with strong positive heat flux. Some of this reduced rate might be due to reduced wind forcing during the middle of the day, and due to stratification effects by bubbles but this can only explain a small fraction of the overall reduction. In Figure 1 the logarithm of the normalized turbulence dissipation rates $\varepsilon/\varepsilon_0$ is plotted versus time in hours relative to the local sunrise, for two depths (0.08 (red) and 1.26 m (blue)). Dissipation rates are normalized by their average rates from -10 hours to -2 hours ε_0 at the specific depth bin. Also plotted with the same x-axis are the measured total heat flux (black), wind stress τ (Wm-2) and the temperature difference between 3 m and 15 m (green), used as a proxy for local stratification in our study. The maximum solar radiation occurred approximately 6 hours after sunrise, while except for 7-8 September (Fig. 1a), the maximum stratification happened 3 hours after that, or 9 hours after sunrise. The breakdown of the stratification coincided with the afternoon/decrease in solar radiation. The scenario on 7-8 September was quite different in that a significant temperature gradient existed between 3 m and 15 m 5 hours before sunrise, decreased around sunrise, and then increased dramatically during the early hours after sunrise. A corresponding drop in the turbulence dissipation rates can be seen during the period from 2 h to 5 h following sunrise (Fig. 1a). Clearly some other process, possibly advection, is added to the general cycle observed on the other days shown in Figure 1. In all cases the turbulence dissipation rates show significantly lower values starting approximately 3 hours after sunrise with minimum values around 11 hours after sunrise on 7-8, 8-9, 9-10 and 10-11 September over the depth range from 0.08 m to 1.26 m. During September 10-11 there is also enhanced near surface turbulence just prior to sunrise and in the early afternoon due to limited periods of increased windstress (Fig. 1d). Generally, the turbulence dissipation rates at 0.08 m and at 1.26 m behave very similar during the hours before sunrise. However, during the period with reduced turbulence our results show that the level is generally more suppressed near the surface, as can be seen in Figure 1, between 8 and 13 hours after local sunrise (Vagle et al. 2011).

What is the effect of the reduced turbulent kinetic energy on the bubble population and therefore on the optical properties of the water? The average bubble size distributions from stable (positive heat flux) and unstable (negative heat flux) conditions are shown in Figure 2. The results suggest that there may be slightly higher number of bubbles with radii between 20 μm and 200 μm during stable conditions. However, the most significant difference seems to be for bubbles larger than 200 μm, where the numbers are significantly reduced. For bubbles with radii between 8 and 100 μm the slope of the bubble size distribution is proportional to a-3 for both conditions. However, during unstable conditions the slope of the bubble size distribution is closer to a^{-6} for larger bubbles, while for stable conditions this decreases to approximately a^{-11}. (The dash-dotted lines are logarithmic extrapolations to larger bubble radii.) In Vagle et al. (2011) we argue that the reduced vertical velocities associated with reduced turbulence allow the larger bubbles, with larger buoyant rise-speeds, to escape.

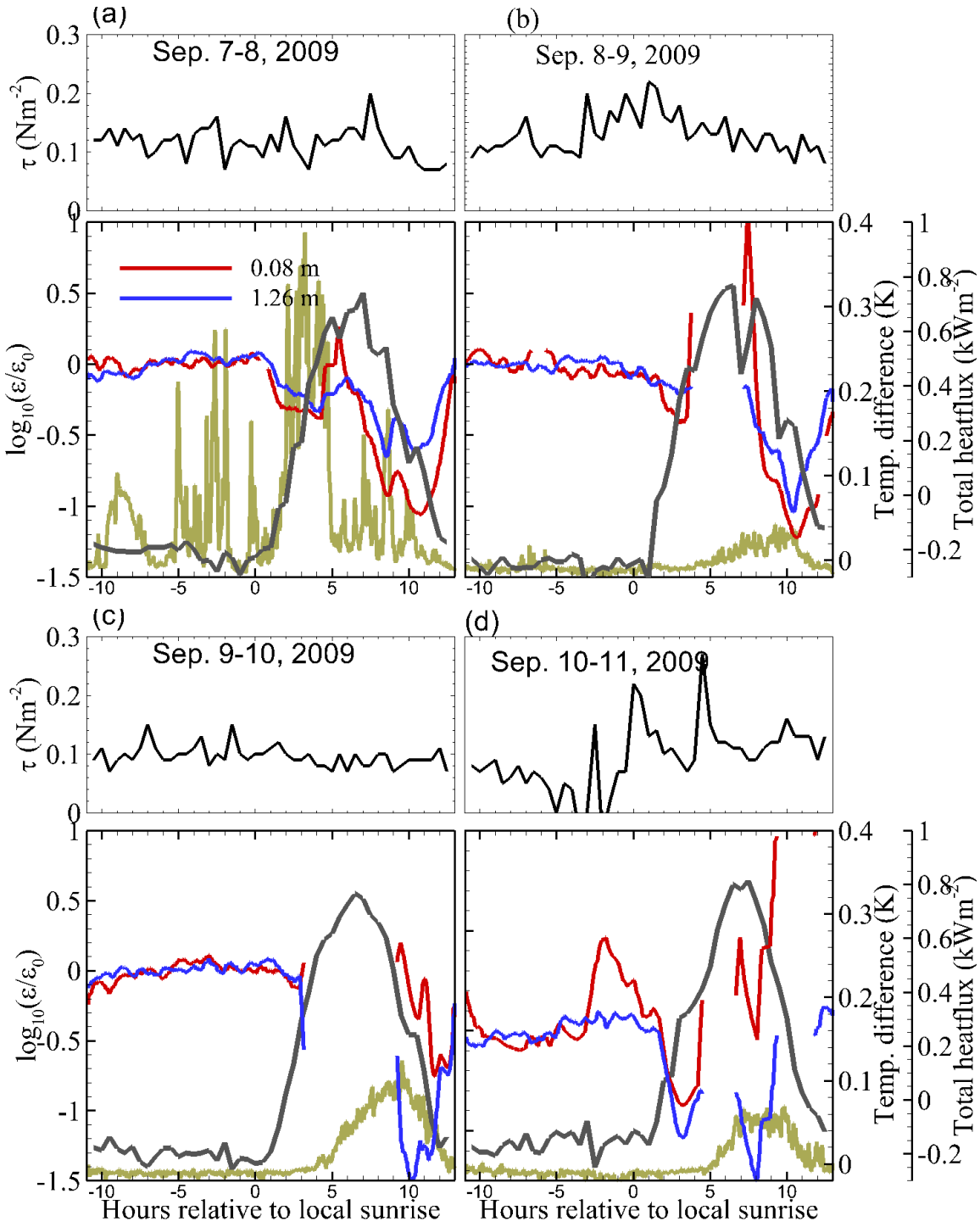

Figure 1. Wind stress,τ, the ratio of turbulent dissipation rate ε normalized by the averaged dissipation rates from -10 hours to -2 hours, ε_0, for two depths (0.08 (red) and 1.26 m (blue)), the total heat flux (black lines), and the temperature difference between 3 m and 15 m (green lines) are plotted versus time in hours relative to the local sunrise for four periods: (a) 7-8 September 2009, (b) 8-9 September 2009, (c) 9-10 September 2009, and (d) 10-11 September 2009.

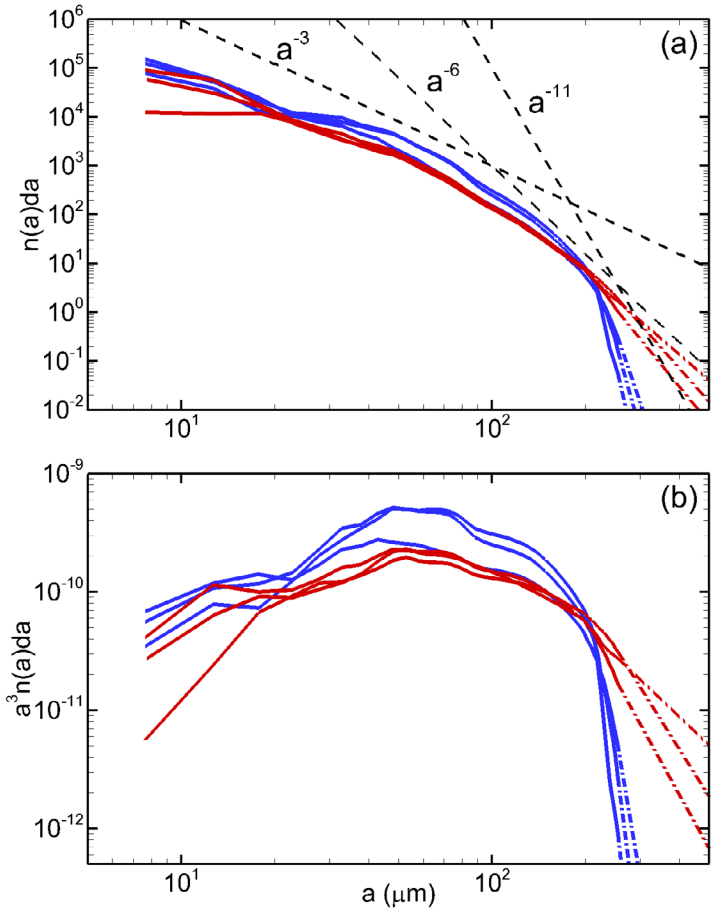

Figure 2. (a) Bubble size distributions averaged over daily periods when the heat flux was positive (stable conditions) (blue lines) and averaged over daily periods with negative heat flux (unstable conditions) (red lines). The dash-dotted lines are logarithmic extrapolations to bubble radii exceeding the current measurement range. Also shown are three different slopes, as discussed in the text (dashed lines). (b) the same distributions scaled by the cubed of the bubble radius.

Light-scattering properties of bubbles suspended in water can be calculated with Mie theory. Following the development by Stramski and Tegowski [2001] one can calculate a volume-scattering cross section due to bubbles, $\sigma_{bub}(\lambda)$, at a given light wavelength λ, and at 0.5 m, the depth of our bubble size distributions, as

$$\sigma_{bub}(\lambda) = \frac{\int_{a=10}^{300} \pi a^2 Q_b(a,\lambda) n(a) da}{\int_{a=10}^{300} n(a) da}, \qquad (1)$$

where $Q_b(a,\lambda)$ is the dimensionless scattering efficiency factor [Bohren and Huffman, 1983] at λ for a bubble with radius a. The integration is performed over the available bubble radii between 10 and

300 μm. Figure 3a shows $\sigma_{bub}(\lambda)$ calculated for a two day period early on in the experiment, showing variability of 3 orders of magnitude in the scattering cross sections at $\lambda = 550nm$. Using both an averaged observed bubble size distribution from this experiment and a bubble size distribution obtained using a 0.9 m distribution from an earlier separate experiment in the Gulf of Mexico, $\sigma_{bub}(\lambda)$ and $\sigma'_{bub}(\lambda)$ were calculated as functions of light wavelength using equation 1 (Fig. 3b). It is clear that due to the omission of the larger bubbles in the present study, the scattering cross section is as much as a factor of 3 lower, at the smallest λ, than in the earlier study. Again choosing a light wavelength of 550 nm, the ratio of the calculated $\sigma_{bub}(\lambda)$ and the predicted $\sigma'_{bub}(\lambda)$ show a ratio of 2 with R^2=0.85 (Fig. 3c).

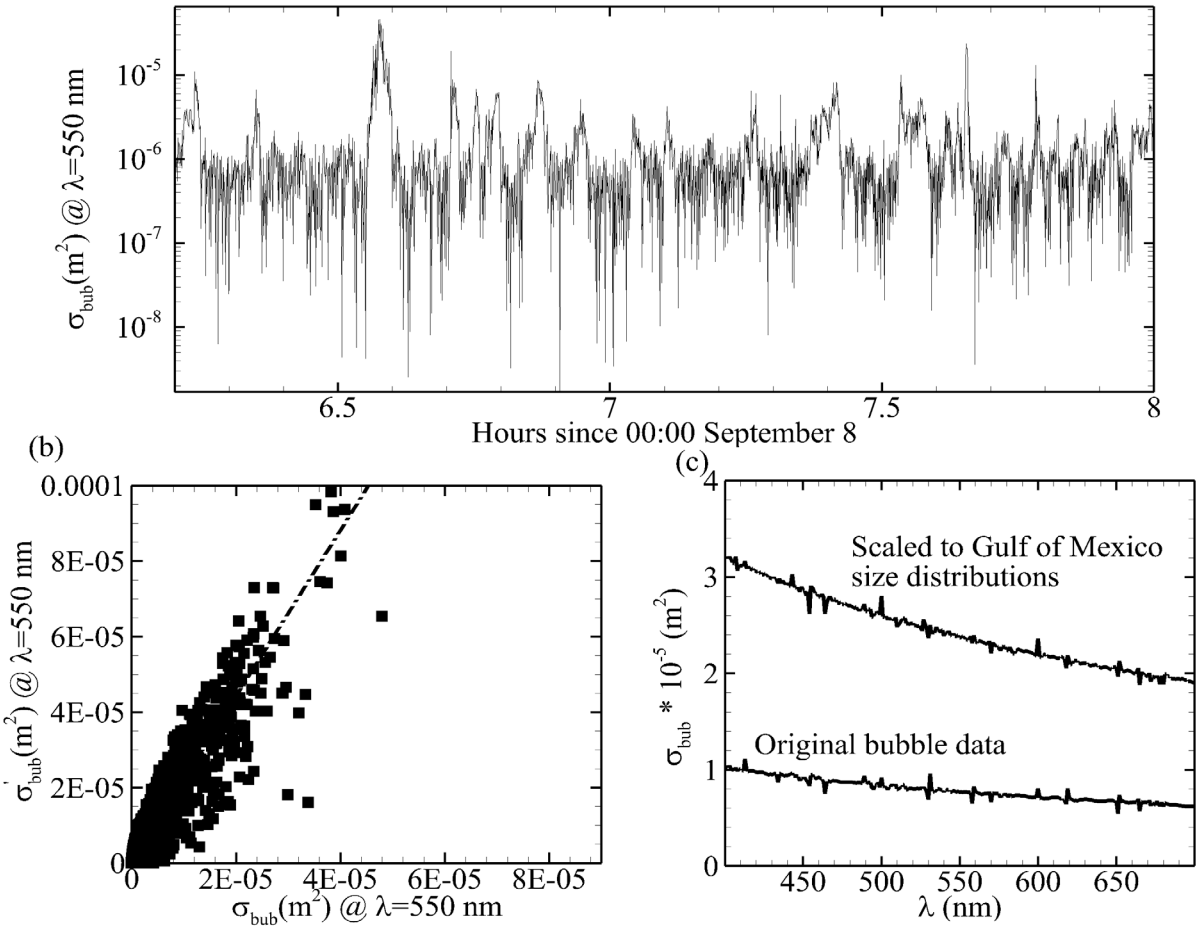

Figure 3. (a) Volume-scattering cross section due to bubbles, σ_{bub} calculated at a light wavelength λ of 550 nm from the bubble size distributions obtained at a depth of 0.5 m for a two hour period on 8 September 2009. (b) σ_{bub} calculated as a function of λ for an averaged bubble size distribution from the RadyO Hawaii study (lower black line) and scaled using size distributions from a Gulf of Mexico experiment (upper black line). (c) σ_{bub} plotted against the volume-scattering cross section due to bubbles calculated using the scaled size distributions, σ'_{bub} at λ=550 nm.

Surfactant measurements in the sea-surface microlayer (SML) during the two ship-based RadyO field studies, combined with similar observations at other sites throughout the world, suggest that this interfacial layer between the ocean and atmosphere covers the ocean's surface to a significant extent (Wurl et al. 2011b). Threshold values at which primary production acts as a significant source of natural surfactants have been derived from the enrichment of surfactants in the SML relative to underlying water and local primary production. Similarly, we have also derived a wind speed threshold at which the SML is disrupted. The results suggest that surfactant enrichment in the SML is typically greater in oligotrophic regions of the ocean than in more productive waters. Furthermore, the enrichment of surfactants persisted at wind speeds of up to 10 m s^{-1} without any observed depletion above 5 m s-1. This suggests that the SML is stable enough to exist even at the global average wind speed of 6.6 m s^{-1}. Global maps of primary production and wind speed are used to estimate the ocean's SML coverage. The maps indicate that wide regions of the Pacific and Atlantic Oceans between 30°N and 30°S are more significantly affected by the SML than northern of 30°N and southern of 30°S due to higher productivity (spring/summer blooms) and wind speeds exceeding 12 m s^{-1} respectively (Wurl et al. 2011b).

Furthermore, the production and fate of transparent exopolymer particles (TEP) has been investigated in various oceanic regions (tropical, temperate and polar), as well from the SML to the deep ocean. TEP accumulation within the mixed layer was observed even in the absence of phytoplankton blooms indicating abiotic processes are important in the production of TEP. The abiotic aggregation rates of TEP measured in the tropical and temperate North Pacific and the Arctic Ocean averaged between 8 and 12 □mol C L^{-1} day^{-1}. Depth profiles from under the Arctic ice revealed the highest TEP concentrations, potentially released from sympagic algal activities at the bottom of the sea ice at the onset of spring. The aggregation rates in the SML were in general enhanced over those in the bulk surface waters by factors of 2 to 30 (Figure 4) (Wurl et al. 2011a). This finding further strengthens a developing consensus on the gelatinous nature of the SML, which will also affect microbial life, light penetration, and surface wave properties (Objective 5).

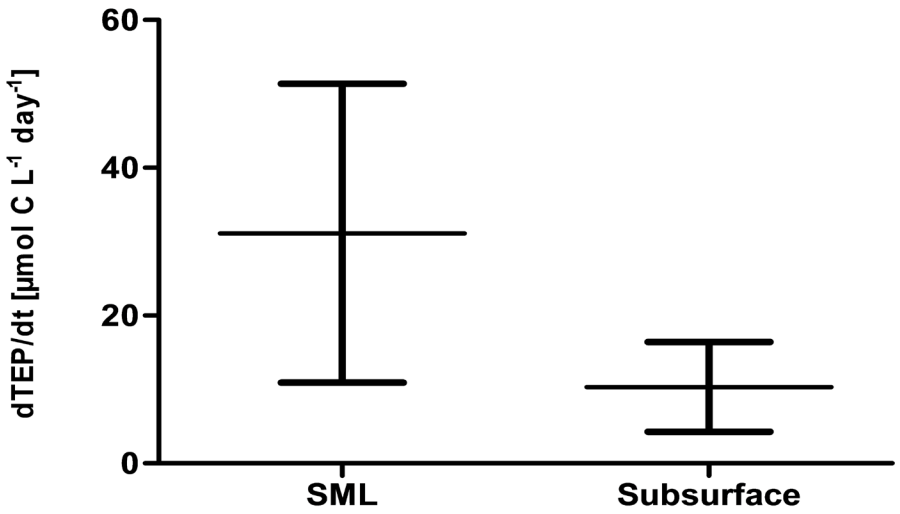

Figure 4. Mean transparent exopolymer particles (TEP) formation rates in the sea-surface microlayer (SML) and subsurface water (1 m depth). The bars represent 95% confidence interval of the mean. The aggregation rates in the SML were in general enhanced over those in the bulk surface waters by factors of 2 to 30.

IMPACT/APPLICATIONS

This effort will provide more detailed information about the presence and number of bubbles and surfactants in the upper ocean and their potential role in optical scatter.

RELATED PROJECTS

Related to other RadyO projects (See website).

REFERENCES

Bohren, C. F., and D. R. Huffman, 1983: Absorption and Scattering of Light by Small Particles, John Wiley, New York.

Farmer, D.M., S. Vagle, and A.D. Booth, 1998, A free flooding acoustical resonator for measurement of bubble size distributions, *J. Atmos. Oceanic Technol.*, 15(5), 1132–1146.

Farmer, D.M., S. Vagle, and A.D. Booth, 2005, Reverberation Effects in Acoustical Resonators for Bubble Measurements, *J. Acous. Soc. Am.,* 118, 2954-2960.

Stramski, D. and J. Tegowski, 2001: Effect of intermittent entrainment of air bubbles by breaking wind waves on ocean reflectance and underwater light field. J. Geophys. Res., 106, 31345-31360.

Terrill, E. & M. Lewis, 2004, Tiny bubbles: and overlooked optical constituent. Oceanography, 11, 11.

Wurl, O., Miller, L., Röttgers, R., Vagle, S. 2009 The distribution and fate of surface-active substances in the sea-surface microlayer and water column, Marine Chemistry 115, 1-9

PUBLICATIONS

Czerski, H., S. Vagle, D. M. Farmer and N. Hall-Patch, 2011a: Improvements to the methods used to measure bubble attenuation using an underwater acoustical resonator. *To appear in J. Acoust. Soc. Am.*

Czerski, H., M. Twardowski, X. Chang, and S. Vagle, 2011b: Resolving size distributions of bubbles with radii less than 30 μm with optical and acoustical methods. Accepted for publication in *J. Geophys. Res.*

Dickey, T. plus 50 authors including S. Vagle, 2011: Recent Advances in the Study of Optical Variability in the Near-surface and Upper Ocean. *Submitted to J. Geophys. Res.*

Twardowski, M., X. Zhang, S. Vagle, J. Sullivan, S. Freeman, H. Czerski, Y. You, L. Bi, and G. Kattawar, 2011: The optical volume scattering function in a surf zone inverted to derive sediment and bubble particle subpopulations. *Submitted to J. Geophys. Res.*

Vagle, S., Gemmrich, J., and H. Czerski, 2011: Effect of upper ocean stratification on turbulence and optically active bubbles. *Submitted to J. Geophys. Res.*

Wurl, O., L. Miller, and S. Vagle, 2011a: Production and Fate of Transparent Exopolymer Particles in the Ocean. *Submitted to J. Geophys. Res.*

Wurl, O., L. Wurl, L. Miller, K. Johnson, and S. Vagle, 2011b: Formation and global distribution of sea-surface microlayers. *Biogeosciences*, 8, 121-135.